

Electric Field Induced Orientation of Polymer Chains in Macroscopically Aligned Electrospun Polymer Nanofibers

Meghana V. Kakade,[†] Steven Givens,[†] Kennecorwin Gardner,[†] Keun Hyung Lee,[†]
D. Bruce Chase,[‡] and John F. Rabolt^{*,†}

Contribution from the Department of Materials Science and Engineering, University of Delaware, Newark, Delaware 19716, and [‡]DuPont CR&D, Wilmington, Delaware 19880

Received July 14, 2006; Revised Manuscript Received November 21, 2006; E-mail: Rabolt@udel.edu

Abstract: The results presented in this work show for the first time that an electric field used to macroscopically align polymer nanofibers can also align polymer chains parallel to the fiber axis. This important result indicates that anisotropic structural properties (mechanical, electrical, etc.) can be induced in polymer nanofibers during the electrospinning process. Such uniaxially oriented nanofibers exhibit a variety of potential applications in biomedicine, microelectronics, and optics. A simple technique of vertical electrospinning with an electric field induced, stationary collection was employed to obtain the molecular orientation in polymer nanofibers. This manuscript describes the orientation process via electrospinning and verifies this molecular orientation in the polymer nanofibers using three independent methods: polarized Fourier transform infrared spectroscopy, polarized Raman scattering, and X-ray diffraction.

1. Introduction

Electrospinning is a versatile process offering unique capabilities for the fabrication (from polymer solutions) of fibers with diameters ranging from the nano- to microscale.¹ The process of electrospinning has already created interesting applications in the filtration of particles smaller than 100 nm in diameter with products in the consumer and defense industry, chemical and biological resistant protective clothing, enzyme or nanoparticle carriers in controlled drug release, wound dressings, scaffolds in tissue engineering,^{2,3} and sensors^{4,5} in electronic applications. A critical need in this field of nanotechnology is the production of uniaxially aligned nanofibers whose anisotropic properties can be tailored for use in microelectronics and in a variety of electrical, optical, mechanical, and biomedical^{6,7} applications. Macroscopic alignment of nanofibers has been successfully accomplished in the past by using different strategies including the use of a scanning tip,⁸ a rotating mandrel collector,^{7,9,10} a copper wire drum,¹¹ and

conducting plates;¹² however, orientation of polymer chains at the molecular level within nanofibers was not observed. Recently, molecular orientation to a small extent along the fiber axis¹³ using a rotating mandrel operating at high rpm (2500) as a collector has been reported. It was hypothesized that mechanical drawing of the fibers caused the molecular orientation. We report, for the first time, molecular orientation in the polymer chains via the use of stationary counter-electrode plates. Hereafter in this paper, the word “alignment” will be associated with the macroscopic alignment of the fibers and the word “orientation” will be associated with the alignment of polymer chains or molecules within the fibers. Two different types of PEO mats; i.e. uniaxially aligned nanofibrous mat and isotropic nanofibrous mat were fabricated via electrospinning. The electrospinning setup and all the parameters used were maintained the same for both the mats except for the way in which the fibers were collected. The fiber alignment reported in this study was confirmed using optical and field emission scanning electron microscopy (FE-SEM). The highly oriented and ordered molecular architecture was determined using polarized Fourier transform infrared spectroscopy (FT-IR), polarized Raman spectroscopy, and wide-angle X-ray diffraction (WAXD).

Electrospinning. The process of electrospinning was first discovered by Formhals in 1934 and improved by different researchers over the years. Many polymers have been routinely electrospun, and several review articles summarizing these have appeared.^{1,14,15} A simple electrospinning apparatus (Figure 1A)

[†] University of Delaware.

[‡] DuPont CR&D.

- (1) Reneker, D. H.; Chun, I. *Nanotechnology* **1996**, *7*, 216–223.
- (2) Yang, F.; Murugan, R.; Wang, S.; Ramakrishna, S. *Biomaterials* **2005**, *26*, 2603–2610.
- (3) Boland, E.; Wnek, G.; Simpson, D.; Pawlowski, K.; Bowlin, G. J. *Macromol. Sci., Pure Appl. Chem.* **2001**, *38*, 1231–1243.
- (4) Wang, A.; Singh, H.; Hatton, T. A.; Rutledge, G. C. *Polymer* **2004**, *45*, 5505–5514.
- (5) Aussawasathien, D.; Dong, J. H.; Dai, L. *Synth. Met.* **2005**, *154*, 37–40.
- (6) Zong, X.; Bien, H.; Chung, C.-Y.; Yin, L.; Fang, D.; Hsiao, B. S.; Chu, B.; Entcheva, E. *Biomaterials* **2005**, *26*, 5330.
- (7) Shields, K. J.; Beckman, M. J.; Bowlin, G. L.; Wayne, J. S. *Tissue Eng.* **2004**, *10*, 1510–1517.
- (8) Kameoka, J.; Orth, R.; Yang, Y. N.; Czaplowski, D.; Mathers, R.; Coates, G. W.; Craighead, H. G. *Nanotechnology* **2003**, *14*, 1124–1129.
- (9) Matthews, J. A.; Wnek, G. E.; Simpson, D. G.; Bowlin, G. L. *Biomacromolecules* **2002**, *3*, 232–238.
- (10) Teo, W. E.; Kotaki, M.; Mo, X. M.; Ramakrishna, S. *Nanotechnology* **2005**, *16*, 918–924.

- (11) Katta, P.; Alessandro, M.; Ramsier, R. D.; Chase, G. G. *Nano Lett.* **2004**, *4*, 2215–2218.
- (12) Li, D.; Wang, Y.; Xia, Y. *Nano Lett.* **2003**, *3*, 1167–1171.
- (13) Fennessey, S. F.; Farris, R. J. *Polymer* **2004**, *45*, 4217–4225.
- (14) Bognitzki, M.; Czado, W.; Frese, T.; Schaper, A.; Hellwig, M.; Steinhart, M.; Greiner, A.; Wendorff, J. H. *Adv. Mater.* **2001**, *13*, 70–72.
- (15) Li, D.; Xia, Y. N. *Adv. Mater.* **2004**, *16*, 1151–1170.

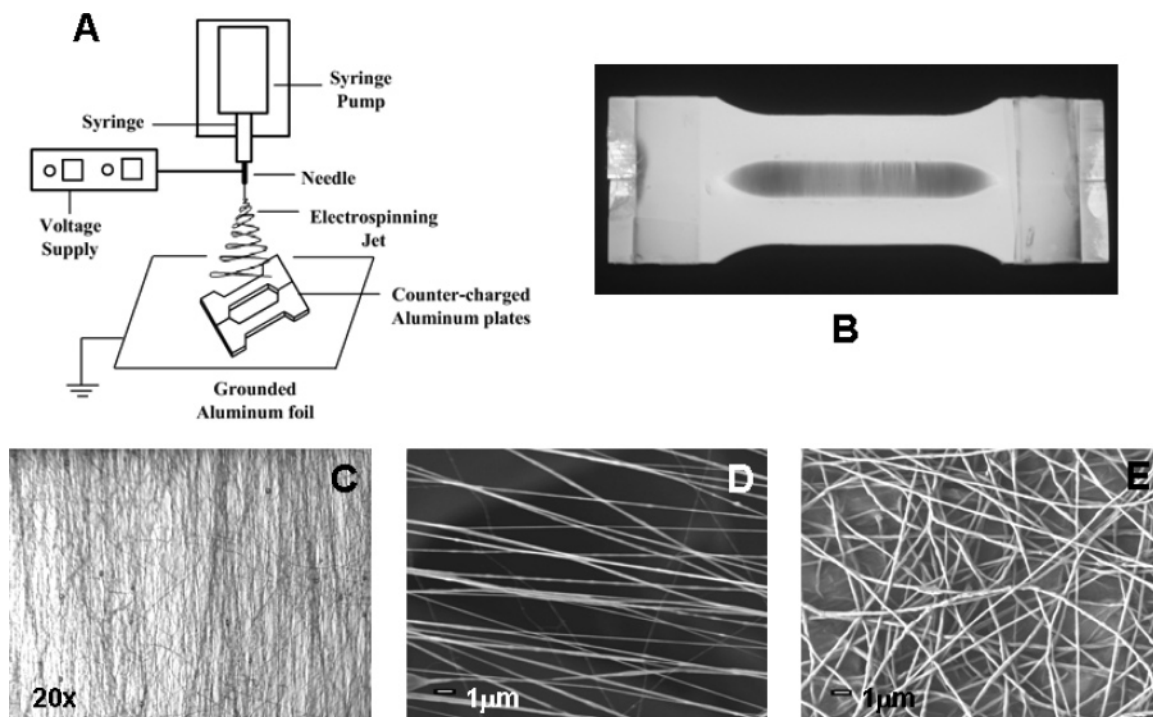


Figure 1. (A) Schematic diagram of electrospinning apparatus; (B) Digital photo of parallel aluminum flat plate collector with aligned fibers; (C) Optical micrograph of aligned PEO nanofibers 20 \times ; (D) FE-SEM image of aligned PEO nanofibers (5000 \times); (E) FE-SEM image of isotropic PEO nanofibers (5000 \times).

consists of three parts—a high voltage supply, a capillary/syringe with a needle, and a grounded collector. The polymer solution is electrically charged by either suspending an electrode in the solution or connecting the electrode to the needle. The applied voltage is usually in the range 1 to 30 kV applied over a distance of 10–30 cm between the syringe tip and the collector. When the electric field is applied, the polymer droplet at the tip of the needle deforms from a hemispherical to conical shape, called a Taylor cone.¹⁶ A jet of polymer emerges from the deformed droplet when the accumulated charge on the droplet surface overcomes the surface tension. The jet begins to stretch and whip around forming a single nanofiber as it travels to the collector. Most of the solvent evaporates during the whipping stage leaving a mostly dry polymer fiber behind. The flow rate of the polymer solution at the syringe tip can be regulated using a syringe pump. The fibers are collected on a counter-electrode or grounded collector. The distance between the needle tip and the collector, called the working distance, can be altered, and the resulting fibers form a random membrane or network on the collector surface. In our electrospinning setup, we have used a set of electrically charged conductive plates with a gap of 1.2 cm between them¹² as a collector. This gap could be altered from a few millimeters to a few centimeters. The electrical charge on the collector plates was maintained opposite to the charge on the polymer solution in order to facilitate and direct the collection of nanofibers on the desired area. Hence, the collector plates served as counter electrodes. The surface morphology can be tailored for specific applications by using different processing conditions¹⁷ and solvents.¹⁸ Electrospinning

has several advantages over conventional melt spinning including a simpler instrumental setup and the use of a smaller amount of material. Electrospun fibers can exhibit nanometer scale diameters, large surface area to mass ratio, large void volumes, an interconnected porous network (for cell migration), and mechanical integrity. Though slow speed and low product volume are its only drawbacks, they do not pose constraints for the process of electrospinning to excel in specific applications.

2. Results and Discussions

A parallel array of fibers was formed consistently in the gap of the negatively charged plates (Figure 1B). The fibers were well aligned as seen from the optical micrograph (Figure 1C). An isotropic nanofibrous mat was formed on the grounded aluminum foil collector. Both types of fiber samples were easily reproduced and removed for characterization purposes. FE-SEM studies were performed in order to investigate the macroscopic alignment of the fibers and to compare the fiber morphology of the aligned fibers (Figure 1D) to that of the isotropic fibers (Figure 1E). In both cases, the fiber surface was observed to be smooth and the fiber diameter was found to be in the range 100 to 400 nm. The lack of change in fiber diameter for the aligned fibers confirmed that there was no physical/mechanical stretching of nanofibers induced by the electric fields associated with the parallel plates, which would have resulted in draw induced narrowing of the fibers.

2.1. Polarized FT–IR Spectroscopy. 2.1.1. Data Analysis. Polarized FT–IR spectroscopy was used to investigate molecular orientation in the nanofibers.¹⁹ Measurements and peak

(16) Taylor, G. *Proc. R. Soc. London, Ser. A* **1969**, 313, 453–475.

(17) Casper, C. L.; Stephens, J. S.; Tassi, N. G.; Chase, D. B.; Rabolt, J. F. *Macromolecules* **2004**, 37, 573–578.

(18) Megelski, S.; Stephens, J. S.; Chase, D. B.; Rabolt, J. F. *Macromolecules* **2002**, 35, 8456–8466.

(19) Hoffmann, C. L.; Rabolt, J. F. *Macromolecules* **1996**, 29, 2543–2547.

(20) Tadokoro, H.; Chatani, Y.; Yoshihara, T.; Tahara, S.; Murahashi, S. *Makromol. Chem.* **1964**, 73, 109–127.

Table 1. PEO Bands and Their Assignments for FT-IR and Raman Measurements^{19–21}

infrared ^a	Raman	assignment (cm ⁻¹)	
		infrared ^a	polarization ^b
2885 m	inactive	$\nu(\text{CH}_2)$	
1342 s		$\omega(\text{CH}_2)$	
1101 vs		$\nu(\text{CO})$	
962 s		$r(\text{CH}_2) + \nu(\text{CH}_2)$	
1448 w	1446 w	$\delta(\text{CH}_2)$	\perp , ZZ
1280 m	1280 s	$t(\text{CH}_2)$	\perp , ZZ
844 s	844 s	$r(\text{CH}_2)$	\perp , ZZ
inactive	1126 m	$\nu(\text{CC})$	
	1064 w	$\nu(\text{CO})$	
	859 w	$r(\text{CH}_2)$	

^a vs = very strong, s = strong, m = medium, w = weak, ν = stretch, r = rock, δ = scissors, ω = wag, t = twist, α = bend. ^b Polarization of IR bands. When a band is both IR and Raman active, then the polarizability tensor element (ZZ) for the Raman experiment is also shown.

assignments were made on three different samples—cast PEO film, a mat of isotropic electrospun PEO nanofibers, and a mat of aligned PEO nanofibers. The PEO bands and their respective assignments are shown in Table 1. The FT-IR spectrum (unpolarized) of cast-film PEO (Figure 2A) was found to be similar to that published by other researchers.²² The polarized FT-IR spectra of isotropic electrospun nanofibers were obtained using two mutually perpendicular polarizations (Figure 2B). The polarized FT-IR spectroscopy of the isotropic fibrous mat indicated random orientation of molecules as the absorbance intensities in relatively perpendicular polarizations were almost identical. This is because, at any polarization angle, the infrared beam encounters almost the same number of C—O—C and C—H bonds and their respective change in dipole moments, resulting in equal absorbance intensities. The FT-IR spectra for isotropic fibers were also similar to the spectra for cast PEO film (Figure 2A) indicating that the electrospun fibrous mat, collected on a grounded electrode, was truly isotropic and had similar conformational order. However, very different absorbance intensities were observed for polarized measurements, parallel and perpendicular to the fiber axis in the FT-IR spectra of aligned PEO nanofibers (Figure 2C). The bands (Table 1) attributed to the C—H stretch at 2885 cm⁻¹, C—H wagging at 1342 cm⁻¹, C—O—C stretch at 1101 cm⁻¹, and C—H rocking at 962 cm⁻¹ have higher intensities when the electric vector is parallel to the fiber axis than when it is perpendicular to the fiber axis. This is because, when most of the PEO chains (7/2 helical form) are oriented in a particular direction and the infrared beam polarized along that direction passes through the sample, then the infrared beam encounters a large number of C—O—C bonds and C—H bonds, coupling with their change in dipole moment of their respective vibrations, resulting in higher absorbance intensities in that particular direction. The difference in the absorbance intensities between parallel and perpendicular polarization can be attributed to molecular orientation of the polymer backbones along the polymer nanofibers' axes.

2.1.2. Dichroic Ratio. The extent of uniaxial orientation exhibited by polymer molecules in a material can be measured by using the concept of a dichroic ratio. Dichroic ratio can be calculated using the formula, $R = P_{||}/P_{\perp}$, where R = dichroic

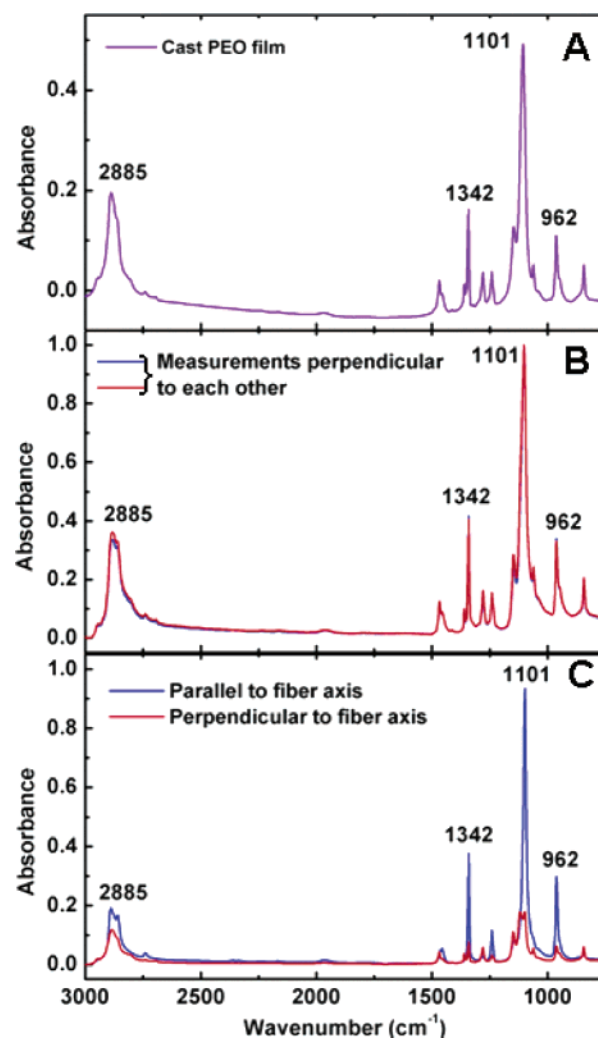


Figure 2. (A) A typical FT-IR spectrum of pure PEO cast film; (B) Polarized FT-IR spectra for isotropic PEO nanofibers show that the peak intensities for two transmission measurements obtained with orthogonal directions of the electric field vector are identical; (C) Polarized FT-IR spectra for uniaxially oriented PEO nanofibers show that the peak intensities for polarized measurements parallel to fiber axis are greater compared to those from the perpendicular measurements.

ratio, $P_{||}$ = parallel-polarized infrared absorbance intensity, and P_{\perp} = perpendicularly polarized infrared absorbance intensity for a particular vibration. For a randomly oriented sample, $R = 1$, and for a uniaxially oriented sample (all polymer chains oriented along the fiber axis and a change in dipole moment of a particular vibration that is co-incident with the fiber axis), $R = \text{infinity}$. Using the polarized FT-IR spectra (Figure 2C), the dichroic ratio for the 1101 cm⁻¹ (C—O—C) band, whose change in dipole moment has a large component along the 7/2 helical backbone, was found to be 5.3. Similarly the dichroic ratios for the other strong “parallel” IR bands at 1342 cm⁻¹ and 962 cm⁻¹ are 5.1 and 5.5, respectively. These results indicate that there is a significant amount of uniaxial orientation of the polymer chains in the PEO nanofibers collected between the charged parallel plates.

2.2. Polarized Raman Spectroscopy. 2.2.1. Data Analysis. Polarized Raman spectra²³ of aligned and isotropic mats of PEO nanofibers were obtained (Figure 3) to confirm the molecular

(21) Yoshihara, T.; Murahashi, S.; Tadokoro, H. *J. Chem. Phys.* **1964**, *41*, 2902–2911.

(22) Hashmi, S. A.; Kumar, A.; Maurya, K. K.; Chandra, S. *J. Phys. D: Appl. Phys.* **1990**, *23*, 1307–1314.

(23) Frisk, S.; Ikeda, R. M.; Chase, D. B.; Rabolt, J. F. *Appl. Spectrosc.* **2004**, *58*, 279–286.

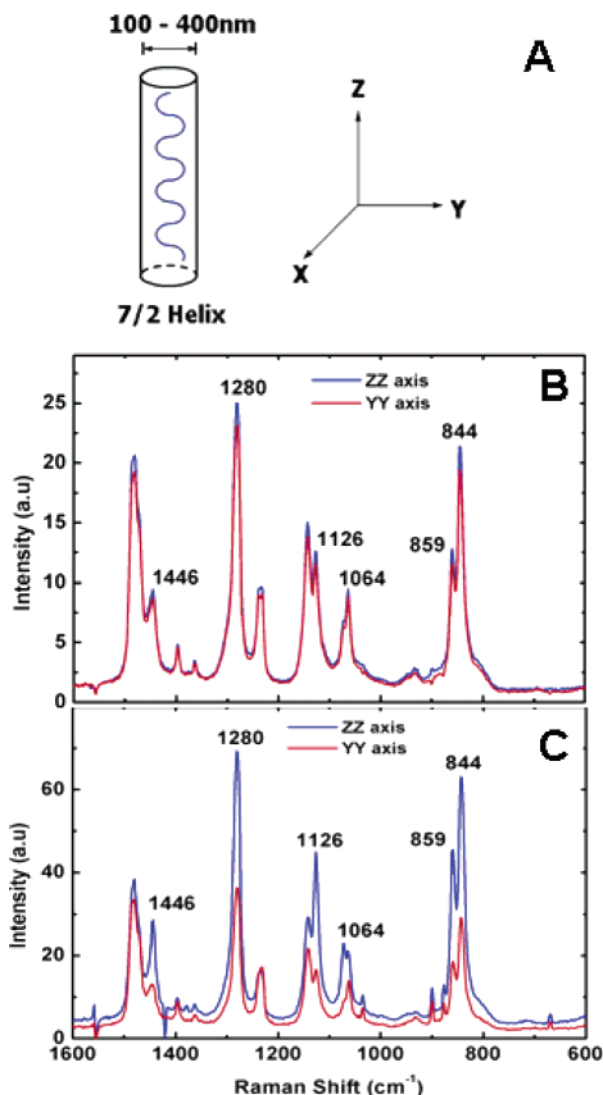


Figure 3. (A) Schematic representation of PEO nanofibers with a 7/2 helical conformation in the polymer backbone and the laser beam axes employed for the polarized Raman spectroscopy experiments; (B) Polarized Raman spectra for the isotropic PEO nanofibers show that the peak intensities of the ZZ measurements were similar to those of the YY measurements; (C) Polarized Raman spectra for the uniaxially oriented PEO fibers show that the peak intensities were greater in the ZZ measurements than the YY measurements.

orientation observed in FT–IR experiments. Polarized Raman spectra with both the incident and scattered polarization vectors parallel to the fiber axis (ZZ) were compared to the spectra obtained with the incident and scattered polarization vectors perpendicular to the fiber axis (YY) for both aligned and isotropic nanofibers. For the isotropic fibers (Figure 3B), the peak intensities of the ZZ polarization were similar to those of the YY polarization, demonstrating that the fibers were truly macroscopically isotropic. However, for the oriented nanofibers (Figure 3C), the peak intensities were greater in the ZZ polarization than in the YY polarization. In particular, the bands (Table 1) attributed to C–H twisting at 1280 cm⁻¹; C–C stretching at 1126 cm⁻¹; C–O–C stretching at 1064 cm⁻¹ and 859 cm⁻¹; and CH₂ rocking at 844 cm⁻¹ have increased scattering intensities in the ZZ polarization compared to the YY polarization indicative of the anisotropic scattering properties of oriented polymer chains.^{24,25} This is because there is a larger

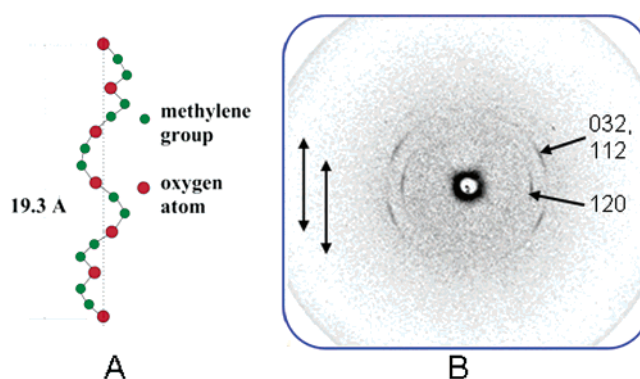


Figure 4. (A) Schematic representation of 7/2 helical conformation of PEO polymer chain,²⁸ corresponding to the orientation direction indicated by the X-ray diffraction pattern. (B) X-ray diffraction pattern of aligned PEO nanofibers showing the sharp X-ray reflections as arcs indicating uniaxially oriented crystals in the nanofibers. The positions of the reflections indicate that the polymer backbones are oriented predominantly along the PEO nanofibers axes, shown by the arrows.

number of polymer chains oriented along the Z direction, and the Raman laser beam (polarized along Z) couples with the change in polarizability for these certain vibrations (totally symmetric symmetry species) predominantly in the ZZ polarization compared to the YY polarization. Hence, uniaxial molecular orientation in the fibers collected between the charged plates was confirmed using polarized Raman spectroscopy.

2.2.2. Molecular Conformation of PEO. Studies have shown that PEO adopts a 7/2 helical molecular conformation^{20,21,26} (Trans–Trans–Gauche) (Figure 4A). This Raman study shows that the PEO still exists in the 7/2 helical form, as the characteristic Raman peaks (1495, 1151, 1041 cm⁻¹) of the planar zigzag form (Trans–Trans–Trans)²⁷ were absent in the spectra of the oriented nanofibers. Also, the dichroic ratios in FT–IR studies were not found to be infinite due to the helical conformation of PEO chains. The conformation of the PEO chains can be affected by many factors such as mechanical stretching, thermal history, solvent evaporation rate, and solvent. The conformation remains unaffected after applying electrostatic forces that have produced chain orientation along the fiber axis. Future studies will focus on the determination of the second (P_2) and fourth (P_4) order orientation functions, using polarized Raman scattering.

2.3. WAXS Pattern and X-ray Diffraction Studies. The sharp X-ray reflections of uniaxially oriented PEO chains along the fiber axis and the indexations²⁹ are shown in Figure 4B. The X-ray diffraction pattern indicates uniaxially oriented crystals in the nanofibers.^{13,21} The chain axes were parallel to the fiber axis, and the reflections appeared to be consistent with the 7/2 helical crystal form of PEO confirming the results of the Raman spectroscopy measurements as discussed above. PEO molecules form 7/2 helical conformation and crystallize in a four-chain monoclinic unit cell ($a = 8.05$ Å, $b = 13.04$ Å, c (fiber axis) = 19.48 Å, and $\beta = 125.4^\circ$). Previous researchers²⁸

(24) Jasse, B.; Koenig, J. L. *J. Polym. Sci., Part B: Polym. Phys.* **2003**, *18*, 731–738.

(25) Kip, B. J.; Vangurp, M.; Vanheel, S. P. C.; Meier, R. J. *J. Raman Spectrosc.* **1993**, *24*, 501–510.

(26) Maxfield, J.; Shepherd, I. W. *Polymer* **1975**, *16*, 505–509.

(27) Ding, Y. Q.; Rabolt, J. F.; Chen, Y.; Olson, K. L.; Baker, G. L. *Macromolecules* **2002**, *35*, 3914–3920.

(28) Takahashi, Y.; Tadokoro, H. *Macromolecules* **1973**, *6*, 672–675.

(29) Mihaylova, M. D.; Kretev, V. P.; Kreteva, M. N.; Amzil, A.; Berlinova, I. V. *Eur. Polym. J.* **2001**, *37*, 233–239.

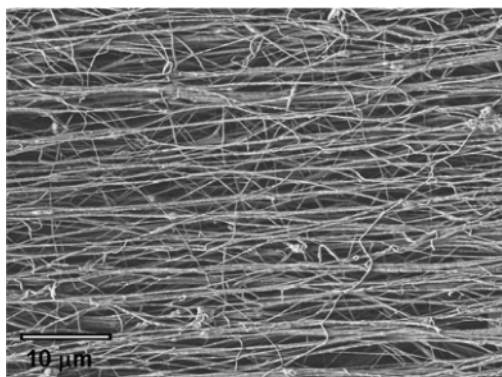


Figure 5. SEM image (2000 \times) of PEO/H₂O nanofibers electrospun on a grounded rotating mandrel. The fibers are aligned at the macroscopic level.

have found that the X-ray intensities could best be fit by a distorted 7/2 helix. When held under tension, the PEO molecule adopts an extended 2/1 helical conformation.³⁰ When tension is released, the molecules relax back into the 7/2 helical conformation.

2.4. Molecular Orientation Comparison: Charged Plates versus Mandrel Collection. Polarized FT-IR and Raman data indicate that the polymer fibers were isotropic when collected on a grounded electrode, whereas the fibers contained uniaxially oriented polymer chains when collected between the charged plates. It was still unclear whether the fibers in the former contained oriented polymer chains originating from the electrospinning process but appeared isotropic due to randomness of the (macroscopic) fibers on the grounded collector. This would also give identical IR spectra in two mutually perpendicular polarizations. So, it was necessary to characterize electrospun nanofibers that would be macroscopically aligned via some other technique. To address this issue, we chose to compare fibers collected on a mandrel with fibers aligned by the electrically conductive plates. The hypothesis being that the molecular orientation occurs due to the effect of electric charge at the edges of the collector plates (Hall Effect) on the polymer chains and not due to the process of electrospinning alone. This was demonstrated by characterizing macroscopically aligned nanofibers, electrospun and collected on a rotating mandrel, using FE-SEM and polarized FT-IR.

PEO/H₂O (8 Wt%) nanofibers were electrospun on a rotating mandrel collector to obtain uniaxially aligned fibers without the effect of an additional external electric field. All the electrospinning parameters were maintained the same as those mentioned in the experimental section except that the collection was done on a grounded rotating mandrel. The mandrel rpm of 1500–1700 was high enough to produce uniaxially aligned fibers and low enough to avoid any mechanical drawing of the fibers, in turn avoiding any polymer orientation. The scanning electron micrograph (Figure 5) indicates that the fibers were macroscopically well aligned.

The polarized FT-IR spectra (Figure 6) show a very little difference in absorbance intensities of the spectra for parallel and perpendicular polarized measurements, indicating a lack of significant molecular orientation in the electrospun nanofibers collected on a mandrel rotating at 1500–1700 rpm. This means that, though the nanofibers were macroscopically aligned, the

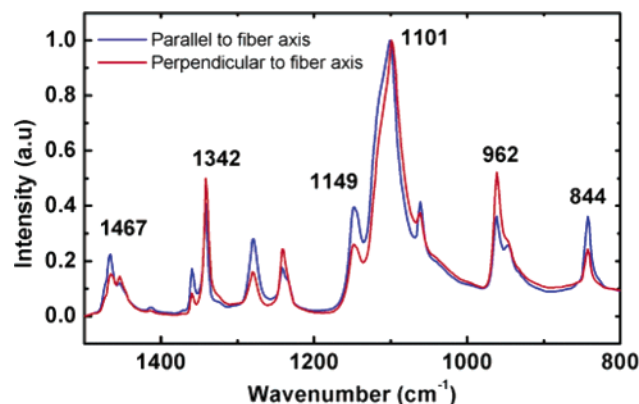


Figure 6. Expanded view of polarized FT-IR spectra from 1500 cm^{-1} to 800 cm^{-1} wavenumbers for PEO nanofibers electrospun on a rotating mandrel. The absorbance intensities in parallel and perpendicular polarizations are very similar to each other. Thus, very little if any molecular orientation of polymer chains is observed, although the fibers were macroscopically aligned as shown in Figure 5.

polymer chains within the nanofibers were not oriented. The polymer chains were isotropic. Since the mandrel was grounded unlike the electrically charged collector plates, the polymer chains had enough time to dissipate the charge and relax by the time the nanofibers were collected on the mandrel. Thus, molecular orientation in the nanofibers was not achieved by electrospinning alone but by electrospinning between the electrically charged plates.

2.5. Discussion of Orientation Mechanism. Water molecules have a strong tendency to align in an induced field because their dipole moment is large, on the order of 80–81 D. In addition the relaxation time of the PEO backbone, which is a measure of how quickly the polymer responds to the orientation induced by the aligning water dipoles, is very close to the relaxation time of water molecules. These comparable relaxation times are unusual. Thus it is possible that the initial alignment of the system is due to the ease of orienting the water dipoles in the electric field used for electrospinning. This alignment of the water dipoles in turn aligns the polymer backbone due to the flexible C–O ether bonds. The negative charge is concentrated at the edges of the collector plates due to the Hall Effect. The positively charged nanofiber acquires the negative charge when it touches the negatively charged edge of the collector plate. These negatively charged nanofibers repel from the like charged collector plates. The fiber alignment in the gap of the aluminum plates occurs due to the hopping back and forth of the nanofibers between the collector plates¹¹ due to charge repulsion. This leaves the water dipoles and PEO chains no time to relax. The system stays under the influence of an induced field throughout this process as the collector is also electrically charged unlike a typically grounded collector (where the fibers get ample time to relax). The electrostatic forces¹² acting on the nanofibers tend to align the fibers with minimal stretching thus allowing the stretched fibers to remain in the stretched state even after removing the film from the plates. The fibrous mat formed could be easily removed for characterization purposes.

Studies on polymer backbone orientation in other polymeric systems and its effect on mechanical, electrical, and optical properties of nanofibers to further explore this result are currently underway.

(30) Takahashi, Y.; Sumita, I.; Tadokoro, H. *J. Polym. Sci., Part B: Polym. Phys.* **1973**, *11*, 2113–2122.

3. Conclusion

PEO polymer backbones within the polymer nanofibers were successfully oriented along the nanofibers axes via electrospinning between two electrically charged aluminum plates. Molecular orientation was not a result of the process of electrospinning alone. Such nanofibers could easily be reproduced and were easy to handle for any characterizations. This method was very simple and did not involve any moving parts, e.g., a rotating collector. The data obtained from the isotropic electrospun nanofibers (collected on a grounded electrode) and oriented electrospun nanofibers was compared and analyzed using FE-SEM, polarized FT-IR spectroscopy, polarized Raman spectroscopy, and X-ray diffraction. Now, we can conclude that a

high degree of orientation of the polymer backbones occurs along the fiber axis via the above-described method.

Acknowledgment. This research was funded by National Science Foundation, DMR 0315461 and DMR 0210223. We sincerely thank Dr. Christopher Snively for his valuable advice on the Raman spectroscopy technique.

Supporting Information Available: Experimental section including material selection and procedures for electrospinning and characterizations. This material is available free of charge via the Internet at <http://pubs.acs.org>.

JA065043F